Beam-Column Design Equations for Wide-Flange Pultruded Structural Shapes

By Ever J. Barbero[1] and Liliana DeVivo[2]

Abstract: A simple procedure is developed for the selection of pultruded structural shapes to be used as beam-columns in structural design. The design equations are then validated by comparison with experimental data gathered during beam-column testing of wide-flange and I-beam pultruded structural shapes. The design procedure accounts for axial load eccentricity and bending action induced by lateral loads and end-moments. The design equations are set in the context of load and resistance factor design, considering both strength and serviceability. This paper addresses the methodology to determine the resistance factors, which should be used with properly selected load-factors accounting for the variability and uncertainty of the loads. The design equations use section-properties, such as the bending stiffness (*EI*), which must be measured and supplied by industry. It is found that the section-properties used in the design of beams and columns are sufficient for the design of beam-columns. Therefore, the cost and time involved in testing structural shapes are minimized. This paper also addresses the means by which section-properties can be generated effectively and inexpensively.

INTRODUCTION

Fiber-reinforced polymer (FRP) structural shapes are produced in standard shapes by pultrusion. The geometry of the cross section and the material properties are fixed by the manufacturer, who offers a broad selection of such structural shapes. Thus, the design carried out by the structural engineer consists of selecting the proper structural shape to carry the loads imposed on a particular member of a structure (frame, truss, etc.). This paper deals with the structural design, or selection, of FRP structural shapes from a given set of available products. Wide flange (WF) and I-sections are used to illustrate the procedure.

FRP columns and beams are being used in a variety of structures, such as buildings, salt storage sheds, bridge superstructures, etc. Design equations for FRP columns and beams are available in the literature (Bank 1989; Barbero and Tomblin 1994; Zureick and Scott 1997). In many applications, columns are also subjected to bending loads. A member that is subject to a combination of axial load and bending moments is called a beam-column (Fig. 1). Bending moments on beam-columns may be caused by transverse loading acting over the member's span, from loading in adjacent members in frames, or by eccentricity of reactions and applied forces in frames. The response of an isolated member to a known system of end forces and moments is considered in this paper. Furthermore, the scope of this paper is limited to the case of eccentricity, lateral load, or end-moment producing bending with respect to the minor axis. Because the structural shapes considered are symmetric about the major axis, no twisting occurs (Galambos 1988; Barbero 1998).

The design of steel beam-columns is addressed by the AISC (1989) and the AISC 1978 Specifications Section 1.6. The design with traditional materials is done using beam-column interaction diagrams that account for the reduction of column load capacity due to bending. Such diagrams do not exist for FRP structural shapes. Therefore, the objective of this paper is to develop design equations and accompanying diagrams to be used by structural engineers in the design of structures using FRP structural shapes.

[1]Assoc. Prof., 315 Engrg. Sci. Build., West Virginia Univ., Morgantown, WV 26506-6106.

[2]Visiting Res. Assoc., West Virginia Univ., Morgantown, WV.

Note. Discussion open until April 1, 2000. To extend the closing date one month, a written request must be filed with the ASCE Manager of Journals. The manuscript for this paper was submitted for review and possible publication on September 29, 1998. This paper is part of the *Journal of Composites for Construction*, Vol. 3, No. 4, November, 1999. ©ASCE, ISSN 1090-0268/99/0004-0185–0191/$8.00 + $.50 per page. Paper No. 19336.

SUPPORTING EXPERIMENTAL DATA

Experimental data, for both concentrically and eccentrically loaded FRP columns, are used in this section to identify the dominant features of the problem. Based on the experimental observations listed below, it is concluded that the main factors controlling the failure of beam-columns are the eccentricity e, column length L, material properties, and geometry of the cross section. An attempt is then made to represent the influence of these parameters into simple design equations.

Concentric Loading

Experimental data from the literature are used here to describe the behavior of columns without eccentricity. Eq. (1), which is plotted with a solid line in Fig. 2, provides a conservative estimate for the buckling load of columns without eccentricity. According to Barbero and Tomblin (1994), the column buckling load is given by

$$P_c = k_i P_L \tag{1}$$

where P_L = short-column load (determined experimentally or numerically as noted in the Design Equations section of this paper); and k_i = interaction factor, given as

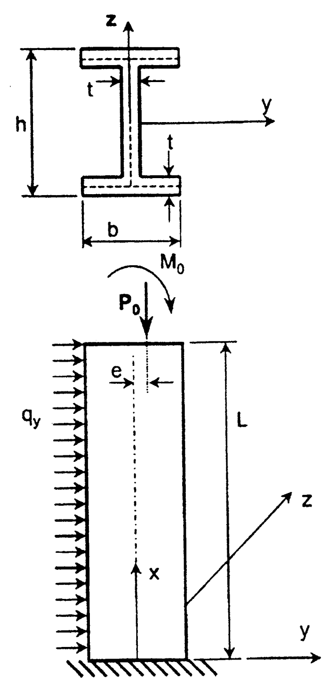

FIG. 1. Beam-Column Geometry and Coordinate System

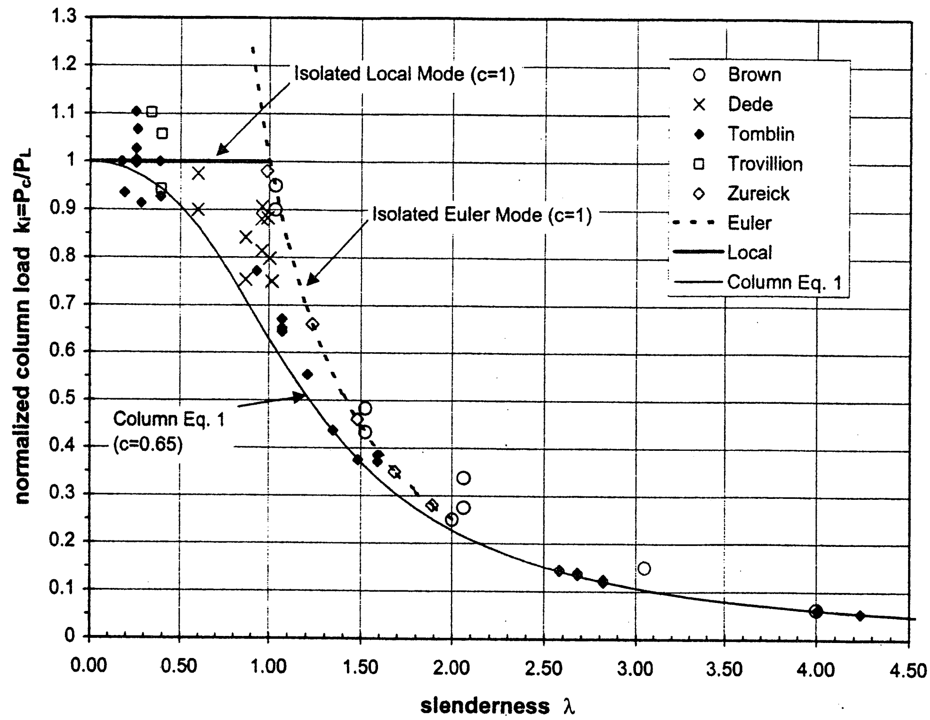

FIG. 2. Failure Loads of Columns Subject to Axial Load without Eccentricity

$$k_i = k_\lambda - \sqrt{k_\lambda^2 - \frac{1}{c\lambda^2}} \tag{2}$$

where the slenderness λ is defined as

$$\lambda = \frac{kL}{\pi}\sqrt{\frac{P_L}{(EI)}} \tag{3}$$

Here, k = end-restraint coefficient; L = length of the column; c = mode-interaction constant; and $k_\lambda = (1 + 1/\lambda^2)/2c$ = intermediate factor introduced to facilitate the computations. As shown in Fig. 2, (1) provides a conservative estimate to the data from Barbero and Tomblin (1994), Zureick and Scott (1997), Barbero and Trovillion (1998), Brown et al. (1998), and Barbero et al. (1999), when the mode-interaction constant is set to c = 0.65. The classical local and Euler curves are recovered by setting c = 1. Note the strong dependency on the slenderness of the column. Also note that the material properties are introduced through the bending stiffness (EI) and the short-column load P_L, which is a function of both the material properties and the geometry of the cross section. Values of (EI) and P_L were taken from the respective references while constructing Fig. 2. The data in Fig. 2 correspond to different cross sections and manufacturers. It must be noted that data from various sources must be compared in dimensionless form because the material properties of the columns differ among manufacturers and fabrication data, even for the same cross section, a fact that is often overlooked in the literature.

Eccentric Loading

Twenty-four WF pultruded shapes produced by Creative Pultrusions, Inc., were tested under axial load with eccentricity (Table 1). The columns were simply-supported at both ends using the testing equipment described by Barbero and Tomblin (1994). Axial, lateral, and flange deformations were recorded in addition to the load. Complete details of the experimental setup and the experimental observations are presented by Barbero and Turk (1999). The following experimental observations were made.

Twenty-three out of 24 columns tested showed significant development of buckling modes before material failure. The only column to fail by material crushing did so after very large lateral deflection, which would be inadmissible in a practical application due to serviceability constraints. A serviceability design equation is presented later in this paper to cover this aspect.

As expected, load eccentricity results in a nonlinear load-deflection plot, as shown in Figs. 3 and 4. The maximum load of an eccentrically loaded column is reduced significantly as compared with the column load without eccentricity. Lateral deflections δ were measured at the midspan and normalized

TABLE 1. Section Properties Used for Design (Weak Axis)

Section (1)	(EI) (kPa·m⁴) (2)	(GA) (kPa·m²) (3)	P_L (kN) (4)	c (5)	M_{cr} (kN·m) (6)
102 × 102 × 6.35	29.644	5,246.0	226.9	0.65	4.26
152 × 152 × 6.35	89.528	7,763.2	169.8	0.65	5.51
152 × 152 × 9.53	148.925	11,858.9	493.8	0.65	17.83
203 × 203 × 9.53	380.355	16,809.6	369.2	0.65	18.24
203 × 102 × 9.53	49.922	8,626.0	640.5	0.65	7.91

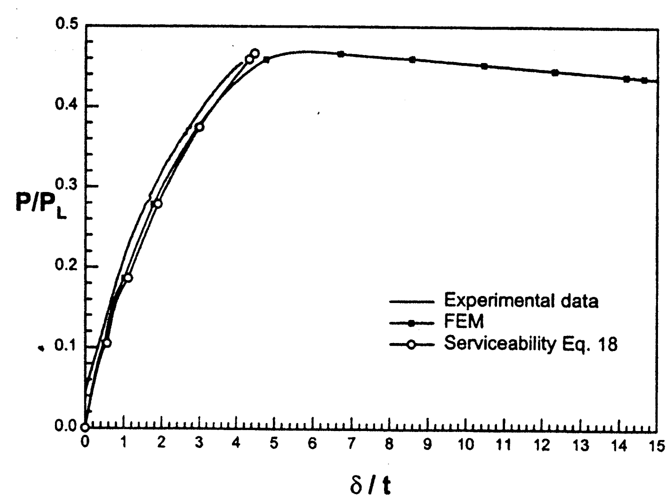

FIG. 3. Load versus Lateral Deflection of WF 203 × 203 × 9.53 mm, L = 3.35 m

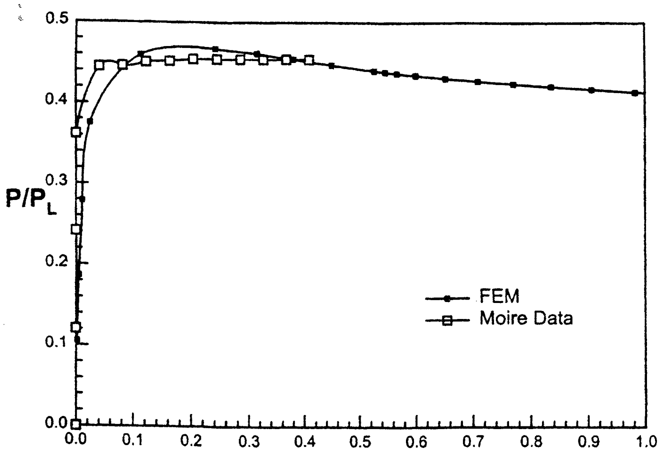

FIG. 4. Load versus Flange Deflection of WF 203 × 203 × 9.53 mm, L = 3.35 m

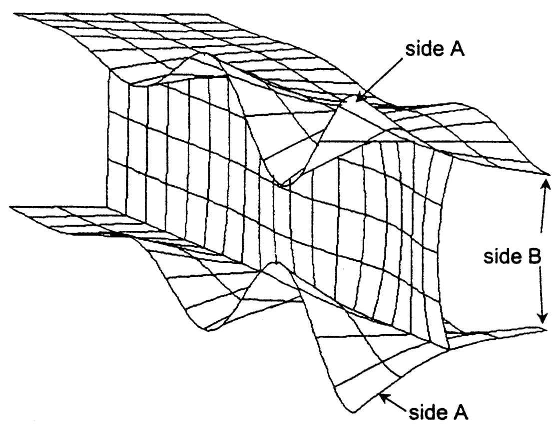

FIG. 5. Deformed Geometry as Predicted by FE Model

by the flange thickness t. The maximum flange deflection occurs at the edge of the flange. This is shown in the finite element (FE) model of an eccentrically loaded column as depicted in Fig. 5. Experimentally, these deflections were measured by an optical technique called shadow moiré (Barbero et al. 1999).

FE SIMULATION

FE modeling was used to consider numerous eccentricities and slenderness, which, due to sample availability, testing equipment, and time constraints, could not be met by testing alone. For example, only eccentricity e = 25.4 mm could be applied in our existing testing setup. Some configurations could not be tested at all. For example, it is relatively simple to introduce load eccentricity in a column test, but it is very difficult to introduce a constant end-moment while the axial load is increased up to failure. For this reason, the design equations for the case of end-moment are based exclusively on FEM simulation. For the simulations to be of value, the model must be verified by experiments. Twenty-four columns were tested for this purpose. The model simulated all aspects of the test setup, including the actual boundary conditions.

The material properties of all the sections tested are reported in Tables 2 and 3 using the coordinate system shown in Fig. 1. The material properties were predicted using micromechanics (Luciano and Barbero 1995). This procedure has been validated experimentally for similar pultruded shapes (Lopez-Anido et al. 1995; Davalos et al. 1996a,b; Qiao et al. 1998) by comparing the predicted material properties with coupon test results.

TABLE 2. Material Properties of Flange for All Sections

Flange (1)	E_x (MPa) (2)	E_y (MPa) (3)	G_{xy} (MPa) (4)	ν_{xy} (5)	t (mm) (6)
102 × 102 × 6.35	26,659	12,921	4,067	0.356	6.35
152 × 152 × 6.35	23,496	12,645	4,012	0.368	6.35
152 × 152 × 9.53	25,373	12,968	4,086	0.357	9.53
203 × 203 × 9.53	28,538	13,769	4,344	0.349	9.53
203 × 102 × 9.53	29,698	14,140	4,458	0.346	9.53

TABLE 3. Material Properties of Web for All Sections

Web (1)	E_x (MPa) (2)	E_z (MPa) (3)	G_{xz} (MPa) (4)	ν_{xz} (5)	t (mm) (6)
102 × 102 × 6.35	22,171	12,158	3,866	0.367	6.35
152 × 152 × 6.35	20,602	11,475	3,674	0.364	7.14
152 × 152 × 9.53	21,798	11,760	3,731	0.363	9.53
203 × 203 × 9.53	22,095	11,861	3,764	0.361	9.53
203 × 102 × 9.53	34,064	16,590	5,327	0.322	9.53

The FE mesh was created by dividing the cross section into 12–16 elements, depending of the type of cross section, and repeating the pattern along the length of the column as many times as necessary to model one-half the column length (Fig. 5). The aspect ratio of all elements was kept equal to one. Symmetry conditions were imposed at the midspan, and multipoint constraints were used to keep the cross section flat but free to rotate at the pinned end, where the load is applied with eccentricity e. Thus, the column bends with respect to the weak axis.

Elements of type SR8 (quadratic, thin-shell, orthotropic) were used (*Abaqus* 1998). An eigenvalue analysis was performed to find the buckling load P_r of columns without imperfections under eccentric load. The Riks method was used to solve the nonlinear problem beyond the maximum post-buckling load P_a for columns with geometric imperfections.

A typical deformed mesh is shown in Fig. 5, displaying results of the nonlinear analysis. Note that both Euler and local modes coexist and interact with each other. It can be seen in Fig. 5 that as a result of lateral deflection (Euler mode), one side of the flanges (side A) has more compression load than the other (side B), which precipitates a local mode (flange deflection). The local mode in turn debilitates the section by reduction of the (EI), as a result of the altered geometry. A reduced (EI) in turn yields more lateral deflection (Euler mode), which feedbacks more load on the compression side of the flange, etc. This is called mode interaction and it has been formally described in the literature (Godoy et al. 1995; Kabir and Sherbourne 1998). The nonlinear analysis performed captures this behavior correctly. The failure load P_a predicted by nonlinear analysis is given by the apex of the load-deflection plot in Fig. 3.

DESIGN EQUATIONS

Perfect Column—Concentric Loading

Based on simulation and experimental results, the effects of various parameters on the failure load were successfully separated as follows. Material properties and geometry of the cross section are accounted for by the bending stiffness of the section (EI), the short-column load P_L without eccentricity, and the mode-interaction coefficient c. These three values can also be used for the design of columns without load eccentricity. In this work, they are considered to be section-properties, independent of the length of the column and the loading conditions. Procedures for the determination of these parameters are available in the literature as follows.

The short-column load P_L can be determined easily by a column test (Tomblin and Barbero 1994). The values should be reported by industry in their design guides. For example, it is reported (*Strongwell*, Section 10, Eq. C-2) that $P_L = 0.5EA/(b/t)^{1.5}$, based on experimental data for their product; A is the area of the cross section, E is the modulus, and b and t are the width and thickness of the flange, respectively. The value of P_L can also be obtained by numerical simulation.

The bending stiffness (EI) can be determined using the procedure described by Bank (1989). The value of (EI) is reported by all pultrusion manufacturers as two factors: E and I. In their design manuals, I is the geometric moment of inertia and E is the apparent modulus obtained by dividing the experimentally measured bending stiffness (EI) by the value of I.

The mode-interaction constant c is easily found (Barbero and Tomblin 1994) from the failure load of a centrally loaded column of critical length [$\lambda = 1$, (3)]. The test is always done with pin-pin end-conditions ($k = 1$), but the resulting failure mode is not Euler buckling. Instead, interaction of local and global modes takes place, which has been proven both theoretically (Godoy et al. 1995; Kabir and Sherbourne 1998) and experimentally (Barbero et al. 1999). If this value is not available, setting $c = 1$ reduces (1) and (2) to the classical case of having two separate equations for stubby and slender columns (see isolated modes in Fig. 2). Barbero and Tomblin reported $c = 0.84$ as the best fit value for their experimental data. From Fig. 2 it is concluded that (1) with $c = 0.65$ provides a conservative estimate for a variety of WF sections from several manufacturers. The interaction constant is used for the design of concentrically loaded columns [(1)] and for the serviceability of beam-columns [(18)].

Perfect Column—Eccentric Loading

To determine the influence of the remaining parameters (eccentricity e and length L), the problem was divided in two. First, the beam-column was assumed to be perfect, that is, without geometric imperfections but with load eccentricity. The buckling load of a perfect column is reduced by the effect of load eccentricity e. The reduced buckling load P_r can be found from a simple eigenvalue analysis (*Abaqus* 1998). Because a perfect column does not exist, no comparison with experimental data can be provided at this point, but a comparison will be provided on the final result. From the simulation it was learned that the normalized buckling load P_r/P_L of a perfect column with eccentricity depends mainly on the ratio e/t. Other factors such as material properties and geometry are accounted for by the value of P_L, which must be determined experimentally from a short-column test without eccentricity (Tomblin and Barbero 1994).

All of the simulation data of five different columns at six different eccentricities and three different lengths are shown in Fig. 6, where $k_r = P_r/P_L$. Some of the data points overlap, partially because the value of k_r is insensitive to the length of the column. A linear regression of the data yields a correlation coefficient of 0.92. This means that 92% of the variability in the data is accounted for by the linear regression in terms of e/t, whereas only 8% is due to factors other than e/t (Montgomery 1991). To account for those undetermined factors and the variability in the data, the design line was traced parallel to the regression line, but leaving all of the simulation data above the line, which yields

$$k_r = 0.871 - 0.0814(e/t) \tag{4}$$

The 95% confidence interval shown in Fig. 6 delimits a region with a 95% probability of containing the linear regression line when a new set of data is used. The lowest of the two 95% lines could be used for design, but, as can be seen in Fig. 6, it would not be conservative for all of the cases

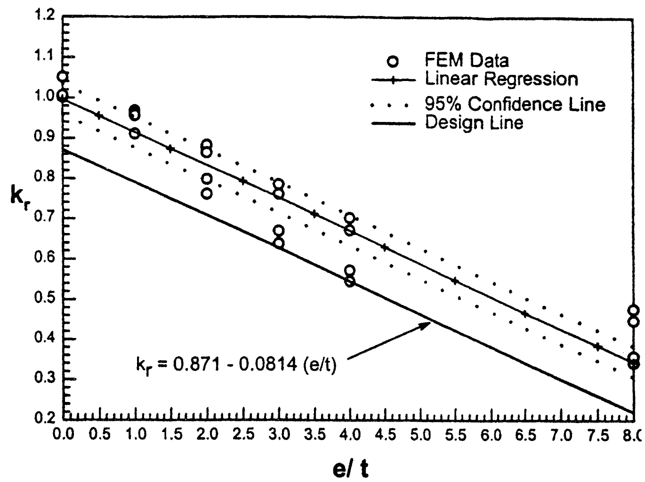

FIG. 6. Resistance Factor to Account for Load-Eccentricity in Case of Eccentric Axial Load (0 < *e/t* < 8). Some Data Points Overlap

considered. Because the chosen design line is below the 95% line, (4) has more than a 95% probability of being conservative.

The design line [(4)] accounts for the eccentricity e/t and the variability of the behavior among the different columns. Therefore, the buckling load of a perfect beam-column can be predicted in terms of the known short-column load P_L as

$$P_r = k_r P_L \tag{5}$$

Eq. (4) is valid within the range $0 < e/t < 8$, for which simulation results were generated. No attempt was made to extend the range further because serviceability clearly controls the design for larger values of eccentricity.

Imperfect Column—Eccentric Loading

The buckling load of a perfect system (e.g., column) provides a good estimate of the actual failure load unless the system is imperfection sensitive, which is the case for a beam-column with eccentricity. In this case a nonlinear analysis accounting for the geometric imperfections is required to estimate the actual failure load. In this work the imperfection was assumed to be in the shape of a linear combination of the local and global modes, both of magnitude $0.25t$, where t is the thickness of the flange. The local and global modes are found by an eigenvalue analysis of the perfect system using the FE model. They are then superposed to the geometry of the column to simulate an imperfect column.

By normalizing the failure load P_a of the imperfect beam-column by the buckling load P_r, it is possible to isolate the influence of slenderness λ on the beam-column behavior. A linear regression of $k_a = P_a/P_r$ in terms of λ (Fig. 7) captures 87% of the variability in P_a over the entire sample population. In this case the sample population consists of five sections, five lengths, and three eccentricities. This means that λ accounts for most (87%) of the changes in P_a/P_r from sample to sample. The remaining 13% of the variability is due to other unknown factors. To take all of the variability into account, a design line is proposed by drawing a line parallel to the regression line, but leaving all of the available data above the line, which yields

$$k_a = 1.102 - 0.644\lambda \tag{6}$$

The design line [(6)] accounts for the slenderness λ and the variability of the behavior among the different columns. Once again, the chosen design line has more than a 95% probability of being conservative. Eq. (6) is valid in the range $0.5 < \lambda <$

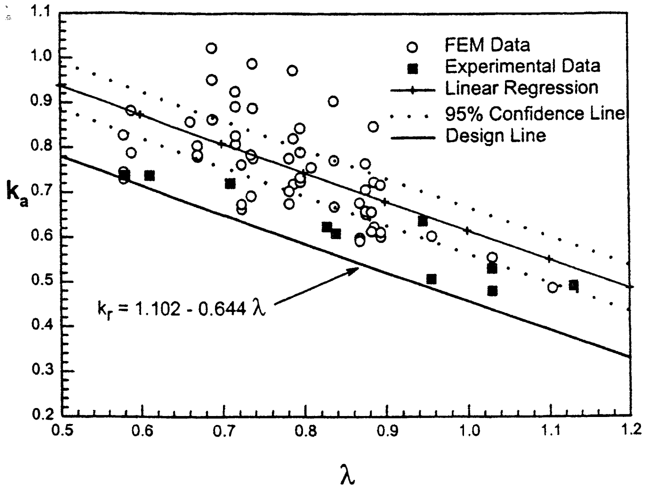

FIG. 7. Resistance Factor to Account for Slenderness in Case of Eccentric Axial Load (0.5 < λ < 1.2). Some Data Points Overlap

1.2, for which simulation results and experimental data were available. No attempt was made to extend the range to high values of slenderness because serviceability controls the design of slender beam-columns, as discussed in the subsection entitled Serviceability. From a design standpoint, k_r and k_a given by (4) and (6), respectively, are resistance factors needed to predict the failure load P_a using the following design equation:

$$P_a = k_r k_a P_L \tag{7}$$

in terms of the short-column load P_L, which should be available in all design manuals provided by industry. Although P_L can be estimated well as the lowest eigenvalue of an FE analysis, it is suggested that, for design purposes, its value be determined experimentally (Barbero and Tomblin 1994).

To validate the procedure summarized by (7), the experimental data were added to Fig. 7. Note that all of the experimental data are above the design line, thus supporting the proposed procedure. Not all of the 24 points can be seen because of some overlap.

The design line is defined using the simulation data. The experimental data are used to corroborate its validity. This method is preferred to the use of experimental data to formulate the design line directly simply because of cost and bias. Experimental data are always limited by the availability of samples (due to its cost), limitations of testing equipment (e.g., only e = 25.4 mm could be tested in our lab), and the cost of testing. Furthermore, new pultruded shapes appear every year and testing them all would be prohibitively expensive. If only limited test data are used, the sample population tends to be biased toward the particular types of sections, sample lengths, or testing variables (e.g., eccentricity) for which more data are available.

A purely experimental study could be formulated and carried out if substantial funds are available. In that case, the design line [(6)] would be based on experimental data. The important point of this work is to show how the effects of material properties, cross-sectional geometry, column length, and eccentricity can be separated and represented by simple design equations.

Lateral Loads

Eq. (7) can also be used for a beam-column subjected to axial and lateral load. First the equivalent end-moment M_0 is computed so that it gives the same maximum deflection on a simply-supported beam as the actual lateral load would give on the beam-column when no axial load is applied and the actual end-conditions are used. The maximum deflection of a beam under a variety of lateral loads and support conditions can be found using standard formulas in terms of the bending stiffness (EI) and shear stiffness (GA) (Barbero 1998, Fig. 8.2). For example, a clamped-clamped beam under a uniform distributed load yields a maximum deflection

$$\delta_{\max} = \frac{qL^4}{384(EI)} + \frac{qL^2}{8(GA)} \tag{8}$$

The shear deformation term in (8) may be significant, even for weak axis bending (up to 17% of the total deflection on some WF sections used in this study, at $\lambda = 1$). Values of (GA) should be reported by the industry, for both weak and strong axis bending.

The equivalent end-moment M_0 is found using the formula for the maximum deflection of a simply-supported column under end moments

$$M_0 = \frac{8(EI)\delta_{\max}}{L^2} \tag{9}$$

where $\delta_{\max}$ is computed by (8). Note that unlike the case of load eccentricity, the end-moment caused by lateral load or transmitted by frame action has a fixed value, independent of the axial load.

The resistance factors for the case of end-moment are found by describing the design lines in Figs. 8 and 9 as

$$k_r = 1.001 - 1.012(M_0/M_{cr}) \tag{10}$$

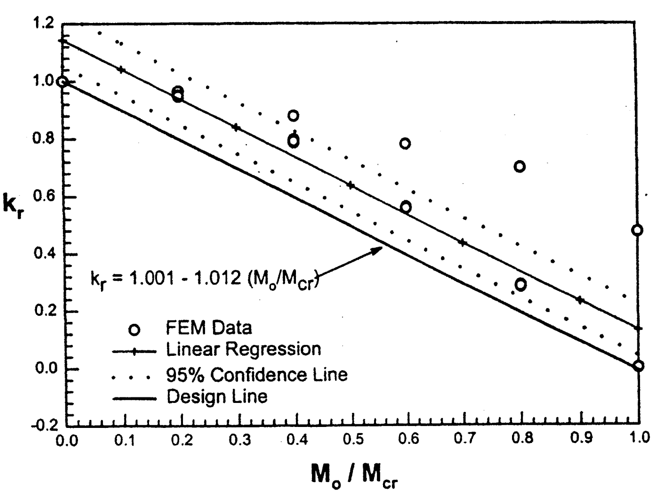

FIG. 8. Resistance Factor to Account for Load-Eccentricity in Case of End-Moment. Some Data Points Overlap

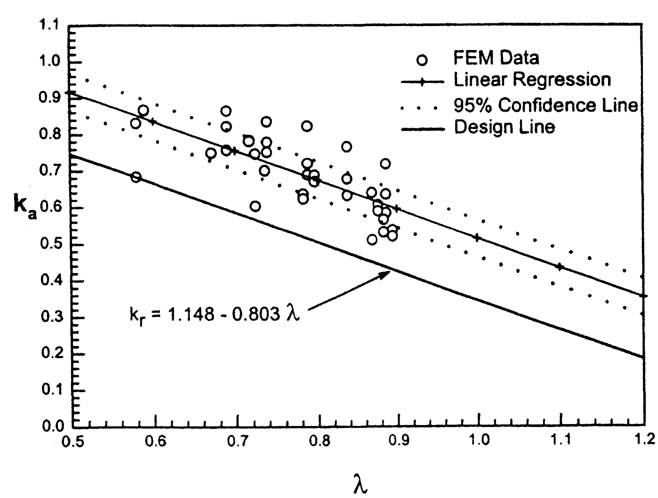

FIG. 9. Resistance Facor to Account for Slenderness in Case of End-Moment (0.5 < λ < 1.2). Some Data Points Overlap

where M_{cr} = ultimate moment of the structural shape under bending load only (Table 1) and

$$k_a = 1.148 - 0.803\lambda \tag{11}$$

In (10), M_{cr} is the actual bending moment at failure of the section tested as a beam, reported by the manufacturer from experimental data or from an accepted prediction methodology.

Serviceability

There are situations when the combination of axial load, load eccentricity, and lateral load will produce excessive lateral deflections, even if the column does not fail. In this case serviceability considerations control the design. Therefore, a serviceability design equation is developed in terms of a reduced bending stiffness, similar to the classical $P - \Delta$ effect for slender columns, which is well known in the literature (Bazant and Cedolin 1991). By taking advantage of (1), the procedure is extended in this section to columns of any slenderness, including short columns. The slenderness λ is defined in (3) for all column lengths.

For a slender column ($\lambda \gg 1$), the column load P_c predicted by (1) approaches the load given by the Euler formula (Fig. 2)

$$P_c \sim P_E = \frac{(EI)}{(kL/\pi)^2} \tag{12}$$

Although the Euler formula can be corrected for shear deformation [divide the result of (12) by $1 + P_E/(GA)$, Gaylord and Gaylord (1972)], the effect is usually small for weak-axis buckling (<4% for all WF sections in this study at $\lambda = 1$).

For a stubby column ($\lambda \ll 1$), the column load P_c given by (1) approaches the short-column load P_L (Fig. 2). However, the load P_c still can be computed by the Euler formula

$$P_c = \frac{(EI)'}{(kL/\pi)^2} \tag{13}$$

if the equivalent stiffness $(EI)'$ is defined as

$$(EI)' = (kL/\pi)^2 P_c = (EI)\frac{P_c}{P_E} \tag{14}$$

with P_c computed by (1).

In the classical $P - \Delta$ procedure for slender columns (Bazant and Cedolin 1991), it is argued that the bending stiffness can be computed from the Euler load as

$$(EI) = (kL/\pi)^2 P_E \tag{15}$$

When $P < P_E$, the term $(kL/\pi)^2 P$ can be interpreted as a reduction of (EI), so that

$$(EI)'_R = (EI) - (kL/\pi)^2 P \tag{16}$$

The argument follows that when P reaches P_E, $(EI)'_R$ reduces to zero and the column buckles. To extend the $P - \Delta$ procedure to the whole range of slenderness, the same argument is used, but on the equivalent bending stiffness. Multiplying (16) by P_c/P_E as in (14), we get

$$(EI)_R = [(EI) - (kL/\pi)^2 P]\frac{P_c}{P_E} \tag{17}$$

Note that when $\lambda \gg 1$, (17) reduces to the classical (16) by virtue of P_c approaching P_E. Finally, the lateral deflection under combined axial and lateral load is computed as

$$\delta = \frac{M_0 L^2}{8(EI)_R} \tag{18}$$

where M_0 = end-moment computed by (9), equivalent to the lateral load. A comparison between predicted and experimental deflections is shown in Fig. 3.

CONCLUSIONS

FE simulation and statistical methods were used to develop resistance factors that represent a lower bound to the expected beam-column load of WF pultruded shapes. Experimental data were generated and used to validate the proposed design equation. The design procedure is synthesized into two dimensionless load-resistance factors (k_r and k_a). Simple linear equations are developed to compute the resistance factors as functions of the dimensionless load eccentricity e/t and column slenderness λ. The coefficients in the linear equations apply to the set of sections used in this study, which are representative of current pultruded structural shapes. As new shapes appear in the marketplace, the procedure described in this paper can be used by industry to refine the numerical values of the coefficients in the linear equations describing the resistance factors. By using the design equations proposed herein, the structural engineer is concerned with only a few relevant section-properties, all of which are normally provided by industry.

ACKNOWLEDGMENTS

This project was sponsored by the West Virginia Division of Highways under contract RP No. 131. The structural shapes were provided by Creative Pultrusions, Inc.

APPENDIX. REFERENCES

Abaqus user manual. (1998). HKS Inc., Pawtucket, R.I.

AISC manual of steel construction allowable stress design (ASD) design manual. (1989). 9th Ed., Section H1, AISC, Chicago.

Bank, L. C. (1989). "Flexural and shear moduli of full-section fiber reinforced plastic (FRP) pultruded beams." *J. Testing and Evaluation*, 17(1), 40–45.

Barbero, E. J. (1998). *Introduction to composite materials design.* Taylor and Francis, Bristol, Pa.

Barbero, E. J., Dede, E., and Jones, S. (1999). "Experimental validation of buckling mode interaction in intermediate length composite columns." *Int. J. Solid and Struct.*, in press.

Barbero, E. J., and Turk, M. (1999). "Experimental investigation of beam-column behavior of pultruded structural shapes." *J. Reinforced Plastics and Composites*, in press.

Barbero, E. J., and Tomblin, J. (1994). "A phenomenological design equation for FRP columns with interaction between local and global buckling." *Thin-Walled Struct.*, 18, 117–131.

Barbero, E., and Trovillion, J. (1998). "Prediction and measurement of the post-critical behavior of fiber-reinforced composite columns." *Compos. Sci. and Technol.*, 58(8), 1335–1341.

Bazant, C. P., and Cedolin, L. (1991). *Stability of structures.* Oxford University Press, New York.

Brown, N. D., Mottram, J. T., and Anderson, D. (1998). "The behavior of columns for the design of pultruded frames: Tests on isolated centrally loaded columns." *Proc., 2nd Int. Conf. on Compos. in Infrastructure*, 2, 248–260.

Davalos, J. F., Qiao, P., and Barbero, E. J. (1996). "Multi-objective materials architecture optimization of pultruded FRP I-beams." *Comp. and Struct.*, 35(3), 271–281.

Davalos, J. F., Salim, H. A., Qiao, P., Lopez-Anido, R., and Barbero, E. J. (1996). "Analysis and design of pultruded FRP shapes under bending." *Composites*, 27B, 295–305.

Galambos, T. V. (1988). *Guide to stability design criteria for metal structures.* 4th Ed., Wiley, New York.

Gaylord, E. H., and Gaylord. L. N. (1972). *Design of steel structures*, 2nd Ed., McGraw-Hill, New York.

Godoy, L. A., Barbero, E. J., and Raftoyianni, I. (1995). "Interactive buckling analysis of fiber-reinforced thin-walled columns." *J. Composite Mat.*, 29(5), 591–613.

Kabir, M. Z., and Sherbourne, A. N. (1998). "Lateral-torsional buckling of post-local buckled fibrous composite beams." *J. Engrg. Mech.*, ASCE, 124(7), 754–764.

Lopez-Anido, R., Davalos, J. F., and Barbero, E. J. (1995). "Experimental evaluation of stiffness of laminated composite beam elements under flexure." *J. Reinforced Plastics and Compos.*, 14(4), 349–361.

Luciano, R., and Barbero, E. J. (1995). "Formulas for the stiffness of composities with periodic microstructure." *Int. J. Solids and Struct.*, 31(21), 2933–2944.
Montgomery, D. C. (1991). *Design and analysis of experiments*. 3rd Ed., Wiley, New York.
Qiao, P., Davalos, J. F., and Barbero, E. J. (1998). "Design optimization of fiber reinforced plastic composite shapes." *J. Composite Mat.*, 32(2), 177–196.
Strongwell design manual. (1998). Strongwell, Bristol, Va.
Tomblin, J., and Barbero, E. J. (1994). "Local buckling experiments on FRP columns." *Thin-Walled Struct.*, 18, 97–116.
Zureick, A., and Scott, D. (1997). "Short-term behavior and design of fiber reinforced polymeric slender members under axial compression." *J. Compo. for Constr.*, ASCE, 1(4), 140–149.